RECENT RESULTS FROM ARGUS ON WEAK DECAYS OF HEAVY PARTICLES

Henning Schröder
DESY, Hamburg, Germany
(representing the ARGUS collaboration*)

ABSTRACT

Results on weak decays of heavy particles are reported from data accumulated by the ARGUS experiment, operating at around 10 GeV centre-of-mass energies in the DORIS II e^+e^- storage ring at DESY. The decay $D^0 \rightarrow \overline{K}^0\phi$ has been investigated with higher statistics yielding a branching ratio of $Br(D^0 \rightarrow \overline{K}^0\phi) = (1.19 \pm 0.25 \pm 0.34)\%$. B-mesons have been reconstructed in decay modes involving D^{*+}, J/Ψ and Ψ' mesons. The decay $\tau \rightarrow \omega\pi\nu$ has been observed for the first time with a preliminary branching ratio of $Br(\tau \rightarrow \omega\pi\nu) = (1.7 \pm 0.4)\%$.

1. INTRODUCTION

Results from the ARGUS collaboration [1] are reported, based on data taken at the e^+e^- storage ring DORIS II at DESY. Since 1983 a total luminosity of 152/pb has been collected at center-of-mass energies near 10 GeV. These data allow the study of weak decays of charmed particles and τ leptons, produced at all center-of-mass energies, as well as B-mesons from $\Upsilon(4S)$ decays, representing a subsample of 59/pb. In particular, we have investigated in detail the decay $D^0 \to \overline{K}^0\phi$ [2] which can only occur at a substantial rate via flavor annihilation by W-exchange [3](Figure 1). The observation of this channel is of critical importance for our understanding of hadronic weak decays. In addition, we have studied exclusive and inclusive B-decays leading to final states which contain charm, such as $B \to D^* + n\pi$ or $B \to J/\Psi X$. Finally, we report the first observation of the decay $\tau \to \omega\pi\nu$.

2. THE DECAY $D^0 \to \overline{K}^0\phi$.

The decay $D^0 \to \overline{K}^0\phi$ was first observed by the ARGUS Collaboration in 1985 with the unexpectedly large branching ratio of $BR(D^0 \to \overline{K}^0\phi) = (1.43 \pm 0.45)\%$. This showed that indeed the W-exchange diagram is very important, despite the fact that this process should be helicity and color suppressed, and it can probably account for the observed lifetime differences between charged and neutral D-mesons. In view of the importance of the decay $D^0 \to \overline{K}^0\phi$, we have repeated the analysis with a much larger data sample including the luminosity accumulated during 1985. The new ARGUS vertex chamber [4] was operational for about 50/pb of this running, and results in a considerable improvement of the quality, most notably, a 60% increase in the efficiency for reconstructing K_s^0's from secondary vertices.

Using the standard criteria for event selection and particle identification [1,2], we obtain the invariant $K_s^0K^+K^-$ mass spectrum shown in Figure 2, which exhibits a clean D^0 signal of 205 ± 38 events at a mass of (1864.3 ± 1.5) MeV/c^2, with a RMS width σ of (8.1 ± 1.5) MeV/c^2. No further cut is applied. The 2-body contributions to the 3-body decay $D^0 \to \overline{K}^0K^+K^-$ can be determined by investigating the K^+K^- subsystem. By requiring $|M(K_s^0K^+K^-) - M(D^0)| < 2\sigma$ we obtain the K^+K^- invariant mass spectrum shown in Figure 3 (points with error bars). Clearly visible is a prominent ϕ signal at the correct mass with the expected shape. Only the range up to a K^+K^- mass of 1.1 MeV/c^2 is shown, but this region contains most of the signal, namely 184 ± 25 events. The part of the K^+K^- mass spectrum which is not correlated with the $D^0 \to K_s^0\phi$ decay is determined from the sidebands above and below the D^0 (hatched histogram). There is a weak uncorrelated ϕ signal on a phase-space background, but a clear excess exists on the D^0.

A further demonstration that indeed the decay $D^0 \to K_s^0\phi$ has been observed is the distribution of the helicity angle θ, where θ is the angle between the K^+ and the K_s^0 in the rest frame of the ϕ meson. This distribution is shown in Figure 4 for $D^0 \to K_s^0K^+K^-$ decay where the K^+K^- invariant masses lies in the ϕ range. The angular acceptance is proven to be constant in the whole angular range. It exhibits the expected $\cos^2\theta$ behaviour, allowing for only a small K^+K^- s-wave contribution below the ϕ. The dependence on $\cos^2\theta$ is also reflected in the Dalitz-plot (Figure 5) As a final consistency check, we have used D^0 mesons produced in the decay $D^{*+} \to D^0\pi^+$, where $D^0 \to K_s^0K^+K^-$ [5]. We find 52 ± 9 events in the D^{*+} peak (Figure 6). The K^+K^- mass spectrum for these events again shows a strong ϕ peak above a much broader contribution which peaks near threshold and then

falls off rapidly (Figure 7). The hatched histogram in the figure represents the background contribution, as determined from the D^{*+} sidebands. It is evident that one way to describe the non-ϕ contribution to the decay $D^0 \to K_s^0 K^+ K^-$ is with a broad K^+K^- theshold effect, that is by the decay $D^0 \to K_s^0 \delta(980)$.

A fit to the data with two Breit-Wigner resonances for the ϕ and the δ, with fixed masses and widths [6] folded with the known resolution function, describes the observed mass distribution quite well (solid curve in Figure 3). No acceptance corrections have to be applied since the acceptance is constant over the whole K^+K^- mass range. On the basis of this fit and the analysis of the θ distibution, we find that $(47 \pm 7)\%$ of all $D^0 \to K_s^0 K^+ K^-$ decays proceed via $D^0 \to K_s^0 \phi$ and the remaining fraction is compatible with $D^0 \to K_s^0 \delta(980)$. If one restricts this analysis to the ϕ region, with $1.01 < M(K^+K^-) < 1.03$ MeV/c^2, one finds that $(79 \pm 5)\%$ of all events in this range are due to the $D^0 \to K_s^0 \phi$ decay. The branching ratio for the decay $D^0 \to K_s^0 \phi$ can be determined by a comparison with the simultaneously measured, and well established, decay $D^0 \to K_s^0 \pi^+ \pi^-$ [7]. By this means, we find:

$$\frac{Br(D^0 \to K_s^0 \phi)}{Br(D^0 \to K_s^0 \pi^+ \pi^-)} = 0.155 \pm 0.033$$

$$Br(D^0 \to \overline{K}^0 \phi) = (1.19 \pm 0.25 \pm 0.34)\%$$

For the remaining fraction of the $D^0 \to K_s^0 K^+ K^-$ decay which might be completely due to the decay $D^0 \to K_s^0 \delta(980)$, we obtain

$$Br(D^0 \to \overline{K}^0 (K^+K^-)_{non-\phi}) = (0.64 \pm 0.15 \pm 0.18)\%$$

The second error in these branching ratios reflects the uncertainty in the $D^0 \to K_s^0 \pi^+ \pi^-$ branching ratio.

In summary, we have unambiguously proven the existence of the decay $D^0 \to \overline{K}^0 \phi$ with a branching ratio consistent with our previous measurement. The suprisingly large value for the branching ratio implies that soft gluons, needed to overcome colour and helicity suppression, are important in D^0 decays.

3. DECAY OF B MESONS.

The reconstruction of B mesons is of basic importance to understand the features of heavy quark systems. Not only does it result in just the masses of charged and neutral B-mesons, and branching ratios for various decay channels, but it also allows for the possiblity of tagging B mesons for study of the Kobayashi-Maskawa matrix elements, $B^0/\overline{B}^0$ mixing and CP-violation which are of fundamental interest.

Exclusive B decays through channels leading to a D^{*+} meson in the final state have been reconstructed. Specifically, the channels $B^0 \to D^{*+}\pi^-$, $B^0 \to D^{*+}\pi^-\pi^0$, $B^0 \to D^{*+}\pi^-\pi^-\pi^+$, and $B^- \to D^{*+}\pi^-\pi^-$, $B^- \to D^{*+}\pi^-\pi^-\pi^0$ have been used. The D^{*+} is detected via its decay into $D^0\pi^+$, where the D^0 is reconstucted via the channels: $D^0 \to K^-\pi^+$, $K_S^0\pi^+\pi^-$, $K^-\pi^+\pi^0$ and $K^-\pi^+\pi^+\pi^-$. Thus in total, 20 decay chains have been investigated, with 3 B^0 and 2 B^- decay channels. To improve the resolution on the mass of the B mesons we performed mass constraint fits to the intermediate states, that is D^{*+}, D^0, K_s^0 and π^0.

In the search for B candidates, two principal cuts were used:

1 We required the probability calculated for the sum of all χ^2 contributions from particle identification and kinematical fitting to exceed 1%.

2 We performed a beam-energy constraint fit for those B-candidates where $|E(B) - E(Beam)| < 3\sigma$. Such a fit translates the rather good momentum resolution for theeh B mesons into a good mass resolution without biasing the background distribution.

The mass spectrum for events satisfying these requirements is shown in Figure 8. We observe a signal of 71 ± 11 events at a mass of (5275.1 ± 0.8) MeV/c^2 with a width of $\sigma = 4.5$ MeV/c^2. The shape of the combinatorial background was determined from event mixing (Figure 9), wrong charge combinations and from the mass distribution obtained in the continuum below the $\Upsilon(4S)$. It can be described by the form:

$$\frac{dN}{dM} \sim M \times \sqrt{1 - \frac{M^2}{E^2_{beam}}}$$

which is derived assuming the background is uniformly distributed in phase space. The sample can be divided into neutral and charged B mesons (Figures 10 and 11). From separate fits to these distributions, we find 40 ± 8 B^0's with a mass of (5276.2 ± 1.0)MeV/c^2 and 32 ± 7 B^-'s with a mass of (5273.8 ± 1.3)MeV/c^2 . If we discard decay chains with large combinatorical background we find a very clean B sample of about 30 events (Figure 12), which can be used for tagging purposes. A comparison with previously published results on the decays $B^0 \rightarrow D^{*+}\pi^-$ and $B^- \rightarrow D^{*+}\pi^-\pi^-$ from the CLEO collaboration shows strong disagreement. The decay rates which we find for these channels are about an order of magnitude smaller than expected from the CLEO results [8]

The decay B $\rightarrow$ Charmonium + X can only proceed via the spectator diagram shown in Figure 13, and is therefore of interest as a test of colour suppression in B decays. Initial studies from ARGUS [9] gave a branching ratio $Br(B \rightarrow J/\Psi X) = (1.37^{+0.6}_{-0.5})\%$, based on an integrated luminosity of 12/pb on the $\Upsilon(4S)$. With 5 times as much data now available, a more detailed picture of the decay B $\rightarrow$ Charmonium + X can be obtained. Figure 14 shows the invariant mass spectrum for e^+e^- or $\mu^+\mu^-$ pairs for events in the $\Upsilon(4S)$ region. The observed J/Ψ signal of 65 ± 12 events at $M(e^+e^-, \mu^+\mu^-) = (3099 \pm 7)$MeV/$c^2$ yields a (preliminary) new branching ratio $Br(B \rightarrow J/\Psi X) = (1.10 \pm 0.24)\%$, in good agreement with the previous result.

Visible at the mass of the Ψ', is an accumulation of about 5 events from the decay $B \rightarrow \Psi' X$. In order to check this hypothesis, we have studied the invariant $J/\Psi\pi^+\pi^-$ mass spectrum (Figure 15). From the known branching ratio for $\Psi' \rightarrow J/\Psi\pi^+\pi^-$, we expect to find about 5 events, which indeed are observed. On the basis of these numbers, we estimate that $Br(B \rightarrow \Psi' X) \simeq 0.4\%$. Thus, roughly 20% of the decay $B \rightarrow J/\Psi X$ is due to $B \rightarrow \Psi' X$, with the Ψ' decaying to the J/Ψ.

The fact that not all J/Ψ mesons are produced directly might lead to a softer momentum distribution for J/Ψ mesons from inclusive B meson decays. If the light quark in the B meson is treated as a spectator one naively would expect from kinematics that the

momentum spectrum is rather hard, unless dominated by high multiplicity channels. The observed spectrum is in fact surprisingly soft (Figure 16) and not quite consistent with a naive spectator picture.

B mesons can be reconstructed rather efficiently by using the $B \rightarrow J/\Psi X$ decay, since the recoil system X must contain a kaon and only a few π's, phase space being relatively limited. So far, we have reconstructed 9 B meson candidates in 4 different channels (Figure 17).

These first results fom ARGUS on reconstructed B mesons opens the unique possibility to study B mesons by using the tagging technique. Three new decay modes involving D^{*+} mesons have been observed for the first time as well as the decay $B \rightarrow \Psi' X$. In comparison with previously reported results on the decays $B^0 \rightarrow D^{*+}\pi^-$ and $B^- \rightarrow D^{*+}\pi^-\pi-$ we obtain an order of magnitude smaller decay rates.

3. THE DECAY $\tau \rightarrow \omega\pi\nu$

One interesting τ decay, until now unobserved, is the decay $\tau \rightarrow \omega\pi\nu$. This channel is of special importance because it can proceed via a second class axial vector current if the $\omega\pi$ system forms a B(1235) meson, with $J^P = 1^+$ and $I^G = 1^+$. The observation of such a decay, $\tau \rightarrow B(1235)\nu$, would be the first manifestation of a second-class current.

Tau pairs were selected by requiring a 1-3 prong topology, with one π^0 on the 3-prong side and no π^0 on the 1-prong side or one π^0 on the 1-prong side which combines with the charged π to a ρ meson. The resulting $\pi^+\pi^+\pi^-\pi^0$ mass distribution (Figure 18) contains 485 events, with a small background contribution of only 30 events. A plot of the invariant $\pi^+\pi^-\pi^0$ mass for these events shows an ω signal of 121 ± 19 events at a mass of $(783. \pm 3.3)\mathrm{MeV/c^2}$ with an RMS width of $(21\pm3)\ \mathrm{MeV/c^2}$ (Figure 19). This is the first observation of the decay $\tau \rightarrow \omega\pi\nu$. We find that the $\tau \rightarrow \omega\pi\nu$ decay represents $(31\pm6)\%$ of the decay $\tau \rightarrow \pi^+\pi^+\pi^-\pi^0$ decay yielding a (preliminary) branching ratio of $Br(\tau \rightarrow \omega\pi\nu) = (1.7\pm0.4)\%$ by taking the world average for the branching ratio of the decay $\tau \rightarrow \pi^+\pi^+\pi^-\pi^0$ of $(5.3\pm0.5)\%$.

The spin-parity of the $\omega\pi$ system can be determined from the distribution of the angle Ψ, the angle between the normal of the ω decay plane and the direction of the bachelor π in the rest system of the ω. (Figure 20). This distribution is obtained by fitting the number of ω 's in each bin of the angular distribution. It clearly favours a $J^P = 1^-$ assignment. This implies that second-class currents do not dominate the decay $\tau \rightarrow \omega\pi\nu$, and we find an upper limit of 50% at the 90% CL for $J^P = 1^+$ contributions to this channel.

The invariant $\omega\pi$ mass distribution in the decay $\tau \rightarrow \omega\pi\nu$ is obtained in a similar way as the angular distribution (Figure 21). No pronounced structure is visible, especially not in the region of the B(1235) meson.

We conclude that the $\tau \rightarrow \omega\pi\nu$ decay represents a sizeable fraction of the τ decays and that it proceeds mainly by a first class vector current.

REFERENCES

Current members of the ARGUS collaboration are: H.Albrecht, P.Böckmann, U.Binder, G.Harder, I.Lembke-Koppitz, W.Schmidt-Parzefall, H.Schröder, H.D.Schulz, R.Wurth (DESY), J.P.Donker, A.Drescher, U.Matthiesen, H.Scheck,

B.Spaan, J.Spengler, D.Wegener (Dortmund), J.C.Gabriel, K.R.Schubert, J.Stiewe, R.Waldi, S.Weseler (Heidelberg), K.W.Edwards, W.R.Frisken, Ch.Fukunaga, D.J.Gilkinson, D.M.Gingrich, M.Goddard, H.Kapitza, P.C.H.Kim, R.Kutschke, D.B.MacFarlane, J.A.McKenna, K.W.McLean, A.W.Nilsson, R.S.Orr, P.Padley, P.M.Patel, J.D.Prentice, H.C.J.Seywerd, B.J.Stacey, T.-S.Yoon, J.C.Yun (IPP Canada), R.Ammar, D.Coppage, R.Davis, S.Kanekal, N.Kwak (Kansas), B.Boštjančič, G.Kernel, M.Pleško (Ljublijana), L.Jönsson (Lund), A.Babaev, M.Danilov, A.Golutvin, V.Lubimov, V.Matveev, V.Nagovitsin, V.Ryltsov, A.Semenov, V.Shevchenko, V.Soloshenko, V.Sopov, V.Tchistilin, I.Tichomirov, Yu.Zaitsev (ITEP-Moscow), R.Childers, C.W.Darden, Y.Oku (South Carolina), and H.Gennow (Stockholm).

1) H.Albrecht et al. (ARGUS collaboration), Phys.Lett. **134B** (1984) 137 and **150B** (1985) 235.

2) H.Albrecht et al. (ARGUS collaboration), Phys.Lett. **158B** (1985) 525.

3) I.Bigi and M.Fugugita, Phys.Lett. **91B** (1980) 121.

4) K.W.Edwards et al. (ARGUS collaboration), The ARGUS Vertex Drift Chamber, to be published in the Proceedings of the Wire Chamber Conference, Vienna (1986).

5) References to a specific charged state should be interpreted as implying the charge conjugate state also.

6) Particle properties data booklet, Rev.Mod.Phys. **56** (1984) No.2,PartII.

7) D.H.Coward et al. (MARK III collaboration) SLAC-PUB-3818 (1985).

8) R.Giles et al. (CLEO collaboration), Phys.Rev.D **30** (1984) 2279.

9) H.Albrecht et al. (ARGUS collaboration), Phys.Lett. **162B** (1985) 395.

FIGURE CAPTIONS

Figure 1 W-exchange diagram for the decay $D^0 \to \bar{K}^0\phi$.

Figure 2 Invariant $K_s^0K^+K^-$ mass spectrum for events from e^+e^- interactions at center of mass energies around 10 GeV.

Figure 3 Invariant K^+K^- mass spectrum for events with $|M(K_s^0K^+K^-) - M(D^0)| < 16.2\text{MeV}/c^2$ (points with error bars). The hatched histogram gives the contribution which is not correlated with a D^0 meson.

Figure 4 Distribution of the helicity angle Θ in in the decay $D^0 \to K_s^0\phi, \Phi \to K^+K^-$ which is defined by $|M(K_s^0K^+K^-) - M(D^0)| < 16.2\text{MeV}/c^2$ and $|M(K^+K^-) - M(\Phi)| < 6.6\text{MeV}/c^2$. The contribution to this angular distribution which is not correlated with a D^0 meson has already been subtracted.

Figure 5 Dalitz plot for events with $|M(K_s^0K^+K^-) - M(D^0)| < 16.2\text{MeV}/c^2$.

Figure 6 Invariant $D^0\pi^+$ mass spectrum with $D^0 \to K_s^0K^+K^-$.

Figure 7 Invariant K^+K^- mass spectrum in the decay $D^{*+} \to D^0\pi^+$, $D^* \to K_s^0K^+K^-$ (open histogram) and from D^{*+} sidebands (hatched histogram).

Figure 8 Sum of invariant $D^{*+}\pi^-$-, $D^{*+}\pi^-\pi^0$-, $D^{*+}\pi^-\pi^-\pi^+$-, $D^{*+}\pi^-\pi^-$- and $D^{*+}\pi^-\pi^-\pi^0$ -mass spectra from events taken at the $\Upsilon(4S)$.

Figure 9 Invariant $D^{*+} + n\pi$ -mass spectrum obtained by event mixing.

Figure 10 Sum of invariant $D^{*+}\pi^-$-, $D^{*+}\pi^-\pi^0$- and $D^{*+}\pi^-\pi^-\pi^+$ -mass spectra from events taken at the $\Upsilon(4S)$.

Figure 11 Sum of invariant $D^{*+}\pi^-\pi^-$- and $D^{*+}\pi^-\pi^-\pi^0$ -mass spectra from events taken at the $\Upsilon(4S)$.

Figure 12 Invariant $D^{*+} + n\pi$ -mass spectrum for decay chains with low combinatorical background.

Figure 13 Spectator diagram for the decay B → Charmonium + X.

Figure 14 Invariant e^+e^-, $\mu^+\mu^-$ mass spectrum for events taken at the $\Upsilon(4S)$.

Figure 15 Invariant $J/\Psi\pi^+\pi^-$ mass spectrum with $J/\Psi \to e^+e^-, \mu^+\mu^-$.

Figure 16 Momentum spectrum of J/Ψ mesons from $\Upsilon(4S)$.

Figure 17 Sum of invariant mass spectra for the decays $B^0 \to J/\Psi + K^{*0}$ (5 events), $B^0 \to \Psi' + K^+\pi^-$ (1 event), $B^- \to J/\Psi + K^-$ (2 events) and $B^- \to \Psi' + K^-\pi^+\pi^-$ (2 events).

Figure 18 Invariant $\pi^+\pi^+\pi^-\pi^0$ mass spectrum in the decay $\tau^+ \to \pi^+\pi^+\pi^-\pi^0$.

Figure 19 Invariant $\pi^+\pi^-\pi^0$ mass spectrum in the decay $\tau^+ \to \pi^+\pi^+\pi^-\pi^0$.

Figure 20 Distribution of the angle Ψ in the decay $\tau^+ \to \omega\pi^+$.

Figure 21 Invariant $\omega\pi^+$ mass spectrum in the decay $\tau^+ \to \omega\pi^+$.

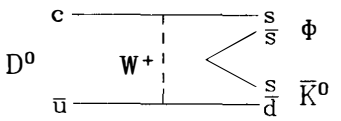

Figure 1

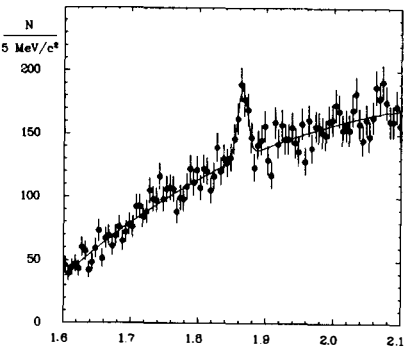

Figure 2

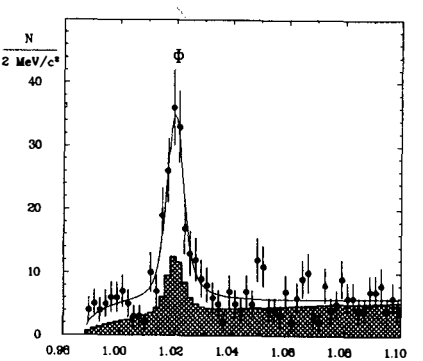

Figure 3

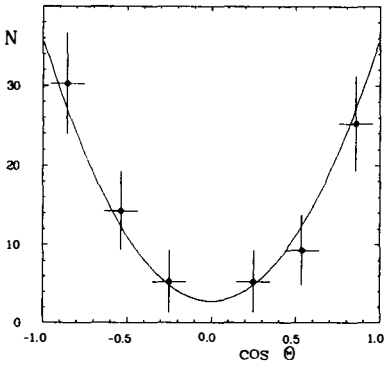

Figure 4

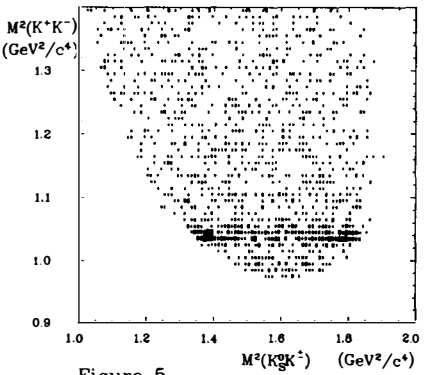

Figure 5

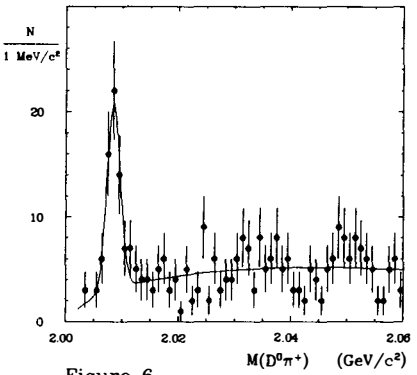

Figure 6

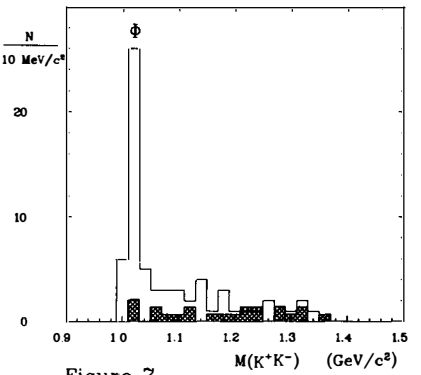

Figure 7

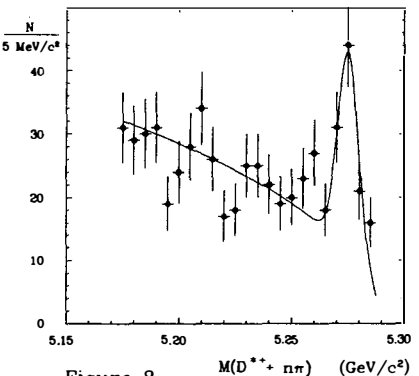

Figure 8

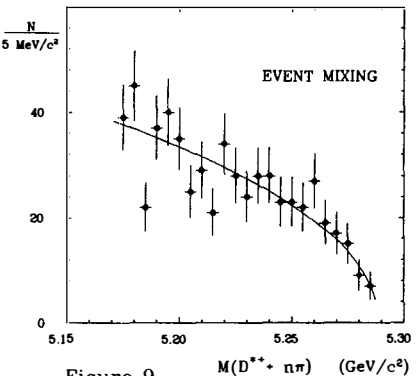

Figure 9

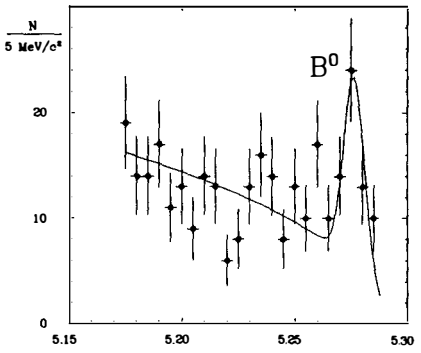

Figure 10

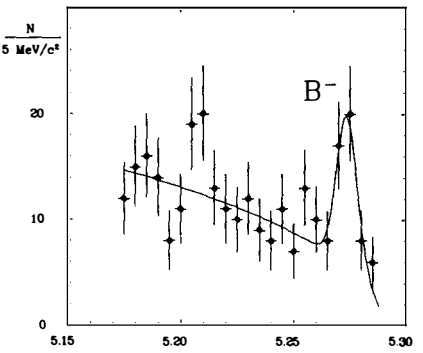

Figure 11

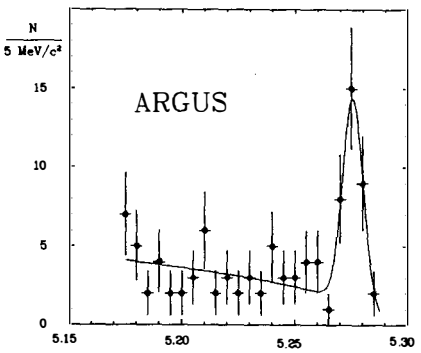

Figure 12

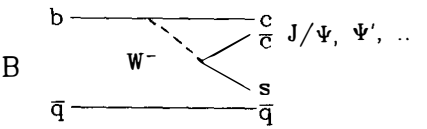

Figure 13

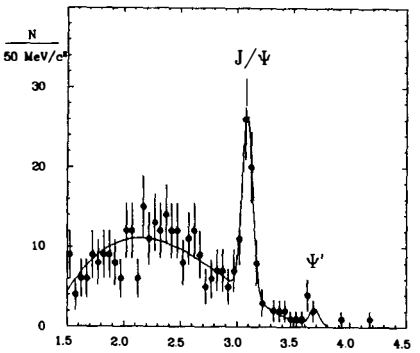

Figure 14

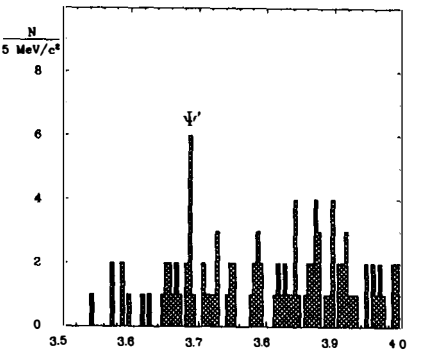

Figure 15

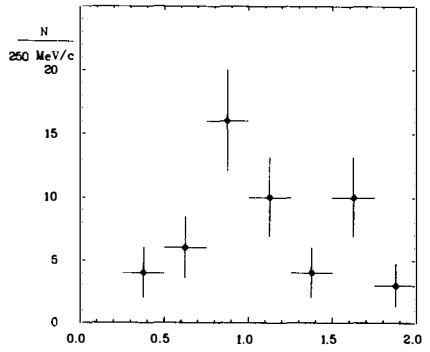

Figure 16

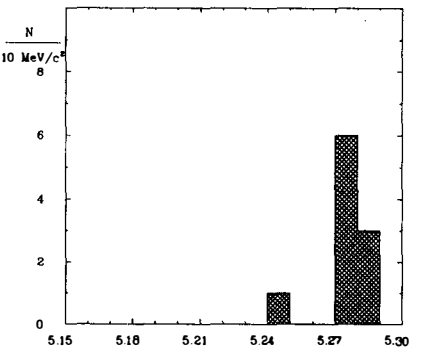

Figure 17

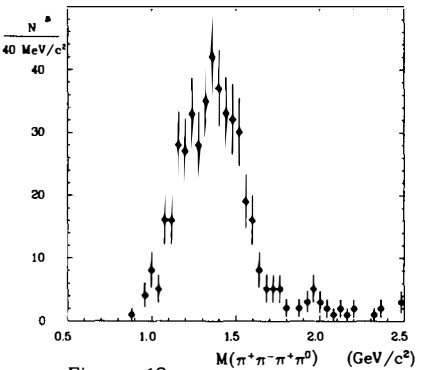

Figure 18

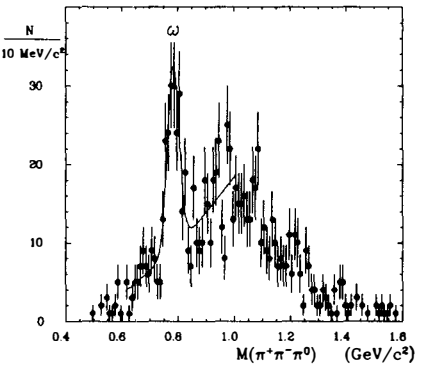

Figure 19

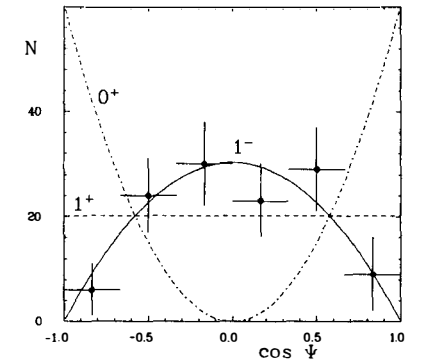

Figure 20

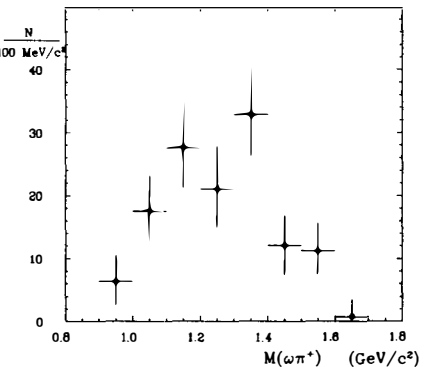

Figure 21